1 # High- and low-temperature pyrolysis profiles describe volatile

2 # organic compound emissions from western US wildfire fuels

4 **Kanako Sekimoto[1,2,3,‡], Abigail R. Koss[1,2,4,*,‡], Jessica B. Gilman[1], Vanessa Selimovic[5],**

5 **Matthew M. Coggon[1,2], Kyle J. Zarzana[1,2], Bin Yuan[1,2,6], Brian M. Lerner[1,2,†], Steven S.**

6 **Brown[1,4], Carsten Warneke[1,2], Robert J. Yokelson[5], James M. Roberts[1], Joost de Gouw[1,2,4]**

8 [1] NOAA Earth System Research Laboratory (ESRL), Chemical Sciences Division, Boulder, CO

9 80305, USA

10 [2] Cooperative Institute for Research in Environmental Sciences, University of Colorado Boulder,

11 Boulder, CO 80309, USA

12 [3] Graduate School of Nanobioscience, Yokohama City University, Yokohama, Kanagawa 236-

13 0027, Japan

14 [4] Department of Chemistry and Biochemistry, University of Colorado, Boulder, CO 80302, USA

15 [5] Department of Chemistry, University of Montana, Missoula, MT 59812, USA

16 [6] Institute for Environmental and Climate Research, Jinan University, Guangzhou, China

17 [*] Now at Department of Civil & Environmental Engineering, Massachusetts Institute of

18 Technology, Cambridge, MA 02142, USA

19 [†] Now at Aerodyne Research, Inc., Billerica, MA 01821, USA

21 [‡]K. Sekimoto and A. Koss are equally contributing first authors.

22 *Correspondence to*: Kanako Sekimoto (sekimoto@yokohama-cu.ac.jp)

25 **Abstract.** Biomass burning is a large source of volatile organic compounds (VOCs) and many

26 other trace species to the atmosphere, which can act as precursors to the formation of secondary

27 pollutants such as ozone and fine particles. Measurements collected with a proton-transfer-

28 reaction time-of-flight mass spectrometer during the FIREX 2016 laboratory intensive were

29 analyzed with Positive Matrix Factorization (PMF), in order to understand the instantaneous

30 variability in VOC emissions from biomass burning, and to simplify the description of these

31 types of emissions. Despite the complexity and variability of emissions, we found that a solution

32 including just two emission profiles, which are mass spectral representations of the relative

33 abundances of emitted VOCs, explained on average 85% of the VOC emissions across various

34 fuels representative of the western US (including various coniferous and chaparral fuels). In

35 addition, the profiles were remarkably similar across almost all of the fuel types tested. For

36 example, the correlation coefficient r of each profile between Ponderosa pine (coniferous tree)

37 and Manzanita (chaparral) is higher than 0.9. We identified the two VOC profiles as resulting

38 from "high-temperature" and "low-temperature" pyrolysis processes known to form VOCs in

39 biomass burning. "High-temperature" and "low-temperature" pyrolysis processes do not

40 correspond exactly to the commonly used "flaming" and "smoldering" categories as described by

41 modified combustion efficiency (MCE). The average atmospheric properties (e.g. OH reactivity,

42 volatility, etc) of the high- and low-temperature profiles are significantly different. We also

43 found that the two VOC profiles can describe previously reported VOC data for laboratory and

44 field burns. This indicates that the high- and low-temperature pyrolysis profiles could be widely

45 useful to model VOC emissions from many types of biomass burning in the western US, with a

46 few exceptions such as burns of duff and rotten wood.

47

48

49 **1 Introduction**

50   Biomass burning is a large source of volatile organic compounds (VOCs) and other trace

51 species to the atmosphere. Reactions involving these VOCs produce ozone and fine particles,

52 which are important air pollutants and radiative forcing agents (Alvarado et al., 2009; Alvarado

53 et al., 2015; Yokelson et al., 2009; Jaffe et al., 2012). Some VOCs from fires also have direct

54 health effects (Naeher et al., 2007; Roberts et al. 2011). Biomass burning occurs in wildfires,

55 controlled burns of wildland and agricultural fuels, and in residential wood stoves and industrial

56 processes. Given the variety of fuels and burning conditions, it is unsurprising that the VOC

57 composition of biomass burning emissions varies greatly between different fire states, locations,

58 and studies. Therefore, it is important to understand VOC emissions from biomass burning in

59 detail and develop a predictive capability that explains some of the variability in VOC emissions.

60   Multiple complex processes take place in biomass burning, including (i) distillation with

61 release of water vapor and terpenes, (ii) pyrolysis of solid biomass giving off flammable gases,

62 (iii) flaming combustion, and (iv) non-flaming processes loosely lumped with smoldering

63 combustion such as glowing (gasification) of biomass (Yokelson et al., 1996; Yokelson et al.,

64 1997; Collard and Blin, 2014; Liu et al., 2016). In a given fire, these processes occur

65 simultaneously, but the relative importance of each process can change with time, which relates

66 to the variability in integrated VOC emissions between different fires. This variability is often

67 parameterized as a function of modified combustion efficiency (MCE = $\Delta CO_2/(\Delta CO + \Delta CO_2)$)

68 (Yokelson et al., 1996). CO_2 and CO are representative gases emitted from the flaming and

69 smoldering combustion processes, respectively, and are measured in most biomass burning

70 studies. MCE is generally higher in flaming combustion (> 0.9) and lower in smoldering

71 combustion (< 0.9) (Akagi et al., 2011).

72   The National Oceanic and Atmospheric Administration (NOAA) led the Fire Influence on

73 Regional and Global Environments Experiment (FIREX) 2016 laboratory intensive conducted at

74 the U.S. Forest Service Fire Sciences Laboratory in Missoula, Montana to study emissions of

75 trace gases and aerosol from wildfires. Emissions from various fuels representative of the

76 western U.S. were sampled under controlled conditions by extensive instrumentation

77 (https://www.esrl.noaa.gov/csd/projects/firex/firelab/instruments.html). Experiments included

78 so-called stack burns, in which emissions from an evolving burn were entrained into a large-

79 diameter stack and sampled by various instruments. VOCs were measured by several instruments,

80 including a PTR-ToF-MS (proton-transfer-reaction time-of-flight mass spectrometer) which

81 captured gas-phase emissions with a fast time response during stack burns. The measurements

82 show variability in VOC composition as the fire shifts between a dynamic mix of distillation,

83 pyrolysis, flaming combustion, and "smoldering" combustion (here we use smoldering as a

84 rough term to include various "non-flame" processes such as gasification). Ions measured with

85 the PTR-ToF-MS were interpreted using a combination of gas-chromatographic pre-separation

86 experiments, literature review, time-series analysis, and comparison to other instruments (Koss et

87 al., 2017). Approximately 90% of the instrument signal could be attributed to identified VOCs.

88   The aims of this work are to understand the variation in gas-phase emissions both over the

89 course of a fire and on a fire-integrated basis, and simplify predictions of the emission of

90 secondary organic aerosol (SOA) and ozone precursors. To do this, the VOCs observed by PTR-

91 ToF-MS in stack burns were analyzed using positive matrix factorization (PMF). We show that

92 much of the observed variability in VOCs can be explained by only two factors: a high-

93 temperature pyrolysis factor and a low-temperature pyrolysis factor, which are named based on

94 the main processes of the VOC emissions from biomass burning. The two factors are compared

95 between fuels. Importantly, the high-temperature factor is quantitatively similar between

96 different fuels, and the same is true for the low-temperature factor. The VOCs present in each

97 factor are discussed in terms of composition, reactivity with OH, and propensity to form

98 secondary organic aerosol. The relative importance of high- and low-temperature pyrolysis

99 factors is quantified for each fuel and discussed with respect to physical properties of the fuel

100 and the burn dynamics. We also investigate how well VOC emissions in biomass burning can be

101 modeled by the two PMF emission profiles through comparisons with previously reported data

102 from laboratory burns and wildfires. Finally, emissions of some specific compounds are

103 discussed.

104

105

2 Methods

2.1 VOC measurements by PTR-ToF-MS

108 Fire emissions were measured during the FIREX 2016 intensive at the Fire Sciences

109 Laboratory in Missoula, Montana. The facility consists of a large combustion chamber and has

110 been described in detail previously (Christian et al., 2003; Christian et al., 2004; Burling et al.,

111 2010).

112 VOC measurements were performed using several instruments, including a PTR-ToF-MS.

113 This instrument employed a high-resolution ToF mass analyzer (Aerodyne Research Inc, MA,

114 USA; Tofwerk AG, Thun, Switzerland) and measured with a time resolution of 2 Hz. VOCs and

115 some inorganic compounds were ionized by proton transfer from H_3O^+ reagent ions. We include

116 the inorganic compounds in the discussion of VOCs. Species with a proton affinity higher than

117 that of water can be measured, which includes many unsaturated and polar compounds. The mass

118 resolution of the instrument (3000-5000 FWHM m/Δm) was sufficient to determine the

119 elemental composition of ions and separate many isobaric compounds. Before each fire,

120 background air in the combustion chamber was measured directly for several minutes. The

121 instrument has been described in detail by Yuan et al. (2016; 2017), and operation, calibration,

122 and peak identification during the FIREX 2016 laboratory intensive were described by Koss et al.

123 (2017).

124

2.2 Fuel and biomass burn descriptions

125
126   Fifteen types of natural fuel mixtures, most of which are representative of important western
127 U.S. ecosystems, were burned. The names below are largely taken from the dominant plant
128 species: (i) Ponderosa pine, (ii) Lodgepole pine, (iii) Loblolly pine, (iv) Douglas fir, (v)
129 Engelmann spruce, (vi) Subalpine fir, (vii) Juniper, (viii) Bear grass, (ix) Ceanothus, (x)
130 Chamise-contaminated, (xi) Chamise-uncontaminated, (xii) Manzanita-contaminated, (xiii)
131 Manzanita-uncontaminated, (xiv) Sagebrush, and (xv) Excelsior (aspen wood shavings).
132 "Contaminated" chaparral fuels (Manzanita and Chamise) were collected from a heavily air-
133 polluted site near San Dimas, CA, while "uncontaminated" fuels were collected from a cleaner
134 site in North Mountain, CA. Individual components of various fuel complexes, including canopy,
135 litter, duff, and rotten wood, were also burned separately. More details on the fires and fuels are
136 given by Selimovic et al. (2017) including: fuel moisture, pre- and post-fire weight, weight of
137 fuel components, and elemental composition (C, H, N, S, and Cl by weight). Each fuel type was
138 burned several times. All fires consumed most of the fuel.

139

140   **2.3 PMF analysis**

141   Measurements by PTR-ToF-MS were analyzed using positive matrix factorization (PMF), a
142 numerical method that can be used to determine major compositional categories of emissions,
143 their compositional profiles, and their relative enhancements over time. PMF was conducted
144 using the PMF Evaluation Tool v. 2.08A (Ulbrich et al., 2009). The basic principles of PMF and
145 application to atmospheric chemistry measurements have been previously described (Ulbrich et
146 al., 2009; Paatero and Tapper, 1994; Paatero, 1997).

147   More than 1000 ions were quantified in the PTR-ToF-MS mass spectra between *m/z* 12-217.
148 Of these, 574 were selected for PMF analysis (Table S2). These 574 ions were resolved from
149 neighboring peaks, were enhanced during at least one fire, and exclude primary (e.g., H_3O^+ and
150 $H_3O^+(H_2O)$) and contaminant ions (e.g., Teflon fragments and transition metals) (Koss et al.,
151 2017). The ion signals (in units of normalized counts-per-second; ncps), which are normalized to
152 the H_3O^+ ion intensities and corrected for ToF-duty cycle, humidity dependence, and H_3O^+ ion
153 depletion as described by Koss et al. (2017), were analyzed using PMF. Typically, raw ion
154 signals in units of "counts-per-second (cps)" have been used for PMF analysis. However, cps

155 VOC ion signals are affected by temporal variability (depletion and instability) in primary ion

156 intensity and humidity during the fire. To obtain PMF results that exclude instrument effects, the

157 normalized and corrected ion signals are used in this analysis. The uncertainties of the

158 normalized and corrected ion signals were calculated based on those originating from the raw

159 (cps) ion signals. We chose to use instrument signal rather than mixing ratio because many ion

160 masses cannot be unambiguously related to a single VOC contributor: they have several

161 contributors, or result from fragmentation, and cannot be converted to mixing ratio. However,

162 variability in these ion signals still contains information useful for PMF. To interpret the PMF

163 results, we did convert to mixing ratio where possible (Section 2.4).

164 In this work, we applied PMF to extended time series, in which all fires of a particular fuel

165 type (e.g., Ponderosa pine) were consolidated into a single data matrix (Figure S1), as well as

166 time series of single fire data. Each fuel type was burned several times. Some individual fires of

167 a particular fuel did not necessarily capture the full possible range of high- and low-temperature

168 fire conditions, because of variability in the relative amounts of fuel parts, fuel moisture content,

169 when fuel was added, or other differences. PMF using the consolidated time series makes it

170 possible to capture the widest possible range of fire conditions. This approach also simplifies the

171 comparison of average emission profiles between different types of fuels. Details on preparation

172 of ion signal and uncertainty datasets are described in the Supporting Information (§1).

173 The discussion in Section 3 is based on the 2-factor PMF solutions. Out of the 574 ions, 434

174 ions were fitted well and together represented 99% of the total ion signal. A total of 140 ions

175 were not well fitted as the difference between their measurements and the PMF reconstruction

176 was higher than 50%; these ions are excluded from the factors presented here. Ulbrich et al.

177 (2009) suggest that poor retrieval of ions with less than 5% of total signal is not uncommon.

178

179 **2.4 Calculations of OH reactivity and volatility**

180 To characterize key chemical properties of the emission profiles derived from PMF analysis,

181 we compare the OH reactivity and volatility of VOCs in each profile. These calculations require

182 conversion of the emission profiles from instrument signal (ncps) to mixing ratio (ppbv).

183 Fragment ions, cluster ions, and ions not well fitted by PMF were excluded from the 574 ions

184 used in PMF analysis and calibration factors were applied to the remaining 400 ions to convert

185 them to mixing ratio. Of these, 156 have known VOC contributors, and account for 90% of the

186   total instrument signal of non-primary and non-contaminant ions between *m/z* 12-217. (This

187   corresponds to an average of 92% of the total VOC concentration detected by PTR-ToF-MS).

188   Details on identification of the VOC contributors to ion masses and calibration are described by

189   Koss et al. (2017).

190   We quantified the importance of the 156 identified ions to OH chemistry by multiplying the

191   VOC + OH reaction rate coefficient (cm^3/molecule/sec) with the VOC fraction in the profile

192   (ppbv VOC/ppbv of total VOC emitted) with a scaling factor to convert from VOC molar

193   emission (ppbv VOC) to number density (molecule/cm^3 at experimental conditions of 900 mbar

194   and 26°C). The resulting OH reactivity is in units of per second per ppbv of total VOCs

195   measured with PTR-ToF-MS (1/sec/ppbv of total VOC emitted). For ions with more than one

196   contributor, a weighted average rate constant was determined. Rate constants were taken from

197   the literature (Atkinson and Arey, 2003; NIST Chemical Kinetics Database; Cicerone and

198   Zellner, 1983; Gilman et al., 2015) or estimated from structurally similar VOCs. Details can be

199   found elsewhere (Koss et al., 2017).

200   We also quantified volatility using the saturation concentration at 25 °C (C_0, μg m^{-3}).

201   Saturation concentrations were taken from the literature (Rumble, 2017-2018; NIST Chemistry

202   WebBook; Yaws, 2015) where possible, and otherwise estimated based on the elemental

203   composition of the ion (Li et al., 2016). Volatility determined from elemental composition is

204   uncertain, especially for compounds with very low volatility where the uncertainty can be several

205   orders of magnitude (Li et al., 2016). We determined volatility for the 400 non-fragmentary ions.

206   We define volatility bins as follows, after Li et al. (2016): volatile organic compounds (VOC, C_0

207   > $3×10^6$ μg m^{-3}), intermediate volatility compounds (IVOC, $300 < C_0 < 3×10^6$ μg m^{-3}), and

208   semivolatile compounds (SVOC, $0.3 < C_0 < 300$ μg m^{-3}). Separation into such volatility bins is

209   commonly used as an aid to discussion of SOA formation potential and gas/particle partitioning

210   (Donahue et al., 2011).

211

212

213   **3 Results and discussion**

214   **3.1 Two-factor parameterization of VOC emissions from biomass burning**

215   Figure 1a shows the time series of selected VOC ion signals from burning a representative

216   mixture of Ponderosa pine fuels. In these lab fires, total VOC emissions (red line in Figure 1a)

217   often increase immediately and substantially during the initial combustion (for 98 seconds after

218   starting the burn in this example), and then total emissions gradually decrease as the flames die

219   out. Emissions of individual VOCs can be seen to fall into two categories: (i) higher emissions

220   during the first part of the fire, e.g. naphthalene, which correlates with the PMF factor we will

221   largely attribute below to high-temperature pyrolysis (blue line in Figure 1a), and (ii) higher

222   emissions during the latter part of the fire, e.g., syringol, which correlates with the PMF factor

223   we will attribute below to low-temperature pyrolysis (green line in Figure 1a). This separation

224   into two categories is typical for most fires, with a few exceptions discussed later (e.g., burns of

225   duff and rotten wood).

226   These two PMF factors (Figure 1b) describe the total VOC emissions remarkably well for

227   most fuels: the differences between the measured ion signals and the calculated ion signals based

228   on the PMF fits are less than 15% on average (Table S1b). For most of the fuels, the time series

229   of the first and second factors are strongly correlated with those of naphthalene and syringol,

230   respectively (correlation coefficient (r) > 0.90). In this work, we primarily attribute these two

231   factors to high-temperature pyrolysis and low-temperature pyrolysis, respectively, and will use

232   these names to describe these factors. The main source of VOC emissions is pyrolysis of fuel

233   biopolymers, and *not* the flaming and/or gasification combustion processes that are described by

234   MCE and often referenced in biomass burning literature. Our association between the factors and

235   pyrolysis temperature is related more rigorously to the distribution of products observed as a

236   function of pyrolysis temperature in the next section. When allowing more than two factors in

237   PMF, the time series and mass spectral profiles of the additional factors can be represented as an

238   "intermediate" or "splitting" of high- and/or low-temperature factors which can be described by

239   a linear combination of the two factors. As examples, Figures S2 and S3 show the correlation

240   between n-factor solutions (n = 3, 4) and PMF results from high- and low-temperature factors for

241   Ponderosa pine datasets. This suggests that only two factors, i.e., high- and low-temperature

242   pyrolysis factors, were needed to explain most of the variability we observed for the VOC

243   emissions from biomass burning.

244   There are notable exceptions to the two-factor solution, including an infrequently observed,

245   but important, third factor that we call a "distillation" factor, and a fourth profile observed during

246   burns of duff. Several fires contain a distillation phase, in which a brief burst of VOCs, typically

247   enriched in terpenes, is emitted immediately prior to ignition. However, PMF captured this phase

248   for only a limited number of burns in which the distillation phase contained sufficient gas-phase

249   emissions and lasted long enough (~30 seconds). When a two-factor solution is used, the

250   terpenes are largely grouped with the high-temperature pyrolysis factor. Duff is defined as a

251   "layer of moderately to highly decomposed leaves, needles, fine twigs, and other organic

252   material found between the mineral soil surface and litter layer of forest soil" (Reardon, 2007).

253   The duff PMF solutions have residuals larger than 80% when solved with only two factors. This

254   means that duff burns have a unique VOC emission pattern that cannot be explained by only

255   high- and low-temperature factors. These exceptions are discussed in more detail later.

256

257   **3.2 VOC emission profiles of high- and low-temperature pyrolysis factors**

258   The mass spectral profiles of the relative abundances of emitted VOCs for the individual

259   PMF factors obtained from a given fuel type are similar for replicate burns of the same fuel type.

260   When comparing the PMF profiles for two individual burns of the Ponderosa pine realistic

261   mixture, the Pearson correlation coefficient (r) is higher than 0.96 for both the high- and low-

262   temperature pyrolysis factors (Figure 2a). Importantly, the mass spectra for the high-temperature

263   pyrolysis factor are also very similar between different fuels, and the same is true for the low-

264   temperature pyrolysis factor. For example, the correlations of each profile between (i) Douglas

265   fir and Ponderosa pine, (ii) Manzanita (chaparral) and Ponderosa, and (iii) Bear grass and

266   Ponderosa have a slope near 1 and $r \geq 0.91$ (Figures 2b-d). In contrast, the correlation between

267   the high- and low-temperature mass spectra is lower ($r < 0.86$ as clearly seen in Figure 2e).

268   Figure 3 shows the average VOC emission profiles of the two factors obtained using PMF results

269   of 15 different fuels. The fractions of individual ion peaks in the emission profiles are

270   summarized in Table S2. These average profiles are in good agreement with profiles of

271   individual fuels: a best fit of $0.96 <$ slope < 1.04 and $r > 0.92$, except for high-temperature factor

272   of Excelsior with $r = 0.83$ (Table S1c and Figure S4). Excelsior is an unusual fuel in that it

273   consists of fine shavings of a single fuel component (wood). VOC composition in high- and low-

274   temperature profiles is discussed in Section 3.3.1.

275   For most emitted VOCs, their relative contributions from the high-temperature versus low-

276   temperature factors are qualitatively related to the temperature of the pyrolysis reactions thought

277   to be the main production mechanism of the VOCs, such as depolymerization, fragmentation,

278   and aromatization (Yokelson et al., 1996; Yokelson et al., 1997; Collard and Blin, 2014; Liu et

279 al., 2016). Figure 4a shows the contribution of each factor to selected pyrolysis products from

280 major fuel biopolymers, i.e., hemicellulose, cellulose, and lignin. The contributions of individual

281 VOCs are expressed by their normalized fractions ($F_{\text{high-T}}$ and $F_{\text{low-T}}$) of high- and low-

282 temperature factors: $F_{\text{high-T}} = Fraction_{\text{high-T}}/(Fraction_{\text{high-T}} + Fraction_{\text{low-T}})$ and $F_{\text{low-T}} =$

283 $Fraction_{\text{low-T}}/(Fraction_{\text{high-T}} + Fraction_{\text{low-T}})$, where $Fraction_{\text{high-T}}$ and $Fraction_{\text{low-T}}$ correspond to

284 fractions (in ppbv/total VOC ppbv) of individual species in the high- and low-temperature VOC

285 profiles (Figure 3), respectively. Figure 4b also shows the relationship between pyrolysis

286 temperature and representative products for individual biopolymers as reported in the literature

287 (Collard and Blin, 2014). During the heating of biomass, different chemical bonds within the

288 biopolymers are broken, which results in the release of VOCs and in rearrangement reactions

289 within the matrix of the residue. Low temperature pyrolysis breaks the bonds between the

290 monomer units of the polymers. Depolymerization in lignin (300-500 °C) produces guaiacols,

291 (iso)eugenol, and syringol. Furans and furfurals are dominantly formed from cellulose and

292 hemicellulose (300-400 °C). These compounds have a higher contribution from the low-

293 temperature factor ($F_{\text{low-T}}$ = 60-100%). Higher temperatures allow reaction of functional groups

294 and covalent bonds in polymers and monomers. The resulting fragmentation emits various

295 VOCs: for example, hydroxyacetone, acetaldehyde, and acetic acid from depolymerization of

296 cellulose and/or hemicellulose. These VOCs have roughly equal contributions from low- and

297 high-temperature factors. The release of oxygenated compounds during depolymerization and

298 fragmentation increases the carbon percentage of the residual biopolymers. Benzene rings and

299 aromatic polycyclic structures form, which is termed char. Higher temperature pyrolysis breaks

300 progressively stronger bonds in char (> 500 °C). This aromatization process gives off aromatic

301 compounds with short substituents (e.g., phenol), non-substituted aromatics (e.g., benzene), and

302 polycyclic aromatic hydrocarbons (PAHs such as naphthalene). Most of those aromatics have a

303 large contribution from the high-temperature factor ($F_{\text{high-T}}$ = 60-100%). As the temperature

304 increases, substituents of the aromatic rings disappear and PAHs are dominantly produced. This

305 is consistent with the contribution of the high-temperature factor to phenol ($F_{\text{high-T}}$ = 60%),

306 benzene (77%), and naphthalene (92%).

307   The VOCs that comprise the two profiles mostly consist of the pyrolysis products described

308 above and their analogs. During a fire, the emissions of any particular VOC can be described by

309 a linear combination of the high-temperature and low-temperature pyrolysis time series. Some

310   VOCs are emitted mainly from the high-temperature pyrolysis; some mainly from the low-

311   temperature profile; and others have a mixed contribution. This is quantified by F_{high-T} as

312   described above. We sorted the VOCs by F_{high-T}, to show how the chemical composition of

313   emissions changes from high- to low-temperature pyrolysis process. Figure 5 shows the chemical

314   characteristics of compounds that are mostly emitted in the high-temperature pyrolysis (F_{high-T} =

315   80-100% in panel (a)), mostly emitted in the low-temperature pyrolysis (F_{high-T} = 0-20% in panel

316   (e)), or have mixed contributions from both pyrolysis (F_{high-T} = 60-80% in panel (b), 40-60% in

317   (c), and 20-40% in (d)). F_{high-T} of each individual VOC is shown in Figure S5. In the category

318   emitted mostly by the high-temperature pyrolysis, important compounds include alkyl-

319   substituted aromatics and aliphatic alkenes (Figures 5a and b), whereas carbonyls have more

320   equal contributions from the high- and low-temperature pyrolysis processes. It should be noted

321   that terpenes (e.g., (oxygenated) monoterpenes and isoprene) emitted from distillation are

322   grouped with the high-temperature pyrolysis (Figures 5a and b; Section 3.6).

323   Several nitrogen (N)-containing compounds also fall into high or low temperature categories

324   consistent with behavior previously reported in the literature. The main N-containing compounds

325   detected by PTR-ToF-MS are isocyanic acid (HNCO), nitrous acid (HONO), hydrogen cyanide

326   (HCN), and ammonia (NH_3). HNCO, HONO, and HCN have a high contribution of the high-

327   temperature factor (F_{high-T} = 80-100% in Figure 5a), while NH_3 falls into the category with a

328   large contribution from the low-temperature factor (F_{low-T} = 86% in Figure 5e). Nitrogen in

329   biomass typically exists as amino acids/proteins and pyrrole/pyridine (aromatic N-heterocycles).

330   During the pyrolysis of those N-functionalities at high temperature (700-1100 °C), HCN is

331   identified as the main product in most cases (Johnson and Kang, 1971; Haidar et al., 1981;

332   Patterson et al., 1968; Houser et al., 1980). NH_3, resulting from the lower-temperature pyrolysis

333   of proteins, has been classified as smoldering combustion gases and falls here into the low

334   temperature profile (Yokelson et al., 1996).

335   The present analysis predominantly focuses on VOCs. The VOC emissions from biomass

336   burning are dominated by pyrolysis reactions of biopolymers. However, this does not mean that

337   emissions of all species are related to pyrolysis. For example, flaming combustion releases CO_2,

338   NO_x, HONO, and black carbon, etc. This is a separate process and cannot be expected to be

339   captured by our VOC framework.

340

3.3 Chemical characteristics of VOC emissions depending on pyrolysis temperature

3.3.1 VOC composition

The VOC emission profiles for the high- and low-temperature factors are shown in Figure 3 and they mainly consist of hydrocarbons, oxygenates with $n=1$-7 oxygen atoms, and nitrogen- and/or sulfur-containing hydrocarbons (Figure 6). In each emission profile, about half of the fraction (in ppbv) is accounted for by a combination of the following seven compounds: (i) ethene (C_2H_4), (ii) formaldehyde (HCHO), (iii) methanol (CH_3OH), (iv) acetaldehyde (CH_3CHO), (v) acrolein (CH_2=CHCHO), (vi) acetic acid (CH_3COOH) and glycolaldehyde ($HOCH_2CHO$), and (vii) ammonia (NH_3). The other half includes several fundamental structures, with a variety of functionalities, as discussed later. Oxygenates with one oxygen are predominant in both emission profiles, accounting for 39% of molar emissions in the high-temperature profile and 36% in the low-temperature profile. Emissions of highly oxygenated compounds (≥ 2 oxygen atoms) and ammonia are higher in the low-temperature profile than in the high-temperature profile. The fractions of hydrocarbons and compounds that contain both N and O, such as HNCO, are lower in the low-temperature profile.

VOCs emitted from biomass burning can be generally organized into major structural groups: furans, aromatics, oxygenated aromatics, aliphatic compounds, and so on. Within each structural category, compounds can have various functionalities, such as alcohol or alkene substituents (Hatch et al., 2015). VOC composition classified by 11 structures and 17 functionalities is shown in Figures 7 and 8. Some VOCs have multiple functional groups. These are counted once in each relevant category. For example, guaiacol is counted in "Oxygenated aromatic" structural category as "Alcohol" and "Ether (methoxy)" functional groups.

The most dominant emissions are attributable to aliphatic oxygenates, i.e., 62% of molar emissions in the high-temperature profile and 60% in the low-temperature profile (Figure 7). This is due to the specific compounds (ii)-(vi) described above. The low-temperature profile is twice as rich in aromatic oxygenates (≥ 2 oxygen atoms) and furans as the high-temperature profile, while the high-temperature profile is enriched in aliphatic (mostly alkenes) and aromatic hydrocarbons. Terpenes (including isoprene, monoterpenes, sesquiterpenes, and oxygenated monoterpenes) emitted from distillation, not from pyrolysis, are dominantly grouped with the high-temperature factor. Compared to the low-temperature profile, the high-temperature profile is enriched in the following functional groups: C-C double bond (>C=C<), C-C triple bond (-

372 C≡C-), diene (>C=C-C=C<), polycyclic aromatic hydrocarbon (PAH), nitrile (-C≡N), amide (-

373 C(=O)-N-), nitro (-NO$_2$), nitrate (-NO$_3$), thiol/sulfide (-S-(H)) (Figure 8). The low-temperature

374 profile is enriched in alcohols (-OH), ethers (mostly methoxy groups: -O-CH$_3$), esters (-C(=O)-

375 O-), and amines (-NH$_2$; mostly ammonia). The emissions of compounds with carbonyl groups

376 (>C=O) and acids (-C(=O)-OH-) are similar. These results are consistent with the contributions

377 of VOC to the high- and low-temperature factors described in Section 3.2.

378

379 3.3.2 OH reactivity

380   The hydroxyl radical (OH) is an important driver of daytime oxidation chemistry.

381 Quantifying the VOC reactivity with OH provides insight into which VOC emissions may be

382 most important for ozone and secondary organic aerosol (SOA) formation. Interestingly, the two

383 profiles have a similar average per-molecule (weighted by abundance) rate constant with OH:

384 15.7×10^{-12} cm^3/molecule/s for the high-temperature profile and 15.8×10^{-12} cm^3/molecule/s for

385 the low-temperature profile. However, the reactivity is provided by very different VOCs in each

386 profile. Aliphatic oxygenates are important in both profiles, but more so in the high-temperature

387 profile (30% of reactivity) than in the low-temperature profile (24% of reactivity). In the high-

388 temperature profile, the reactivity also has a large contribution from terpenes and aliphatic

389 hydrocarbons, while in the low-temperature profile, the reactivity is largely due to furans and

390 aromatics (Figure 9a). Since the total VOC emissions in real-world fires come from a mixture of

391 the high- and low- temperature pyrolysis factors, the total OH reactivity can be estimated from

392 the relative importance of the high- and low-temperature pyrolysis in a given fire.

393

394 3.3.3 Volatility

395   Volatility is another important chemical characteristic affecting secondary organic aerosol

396 (SOA) yield and formation rate. The low-temperature emission profile contains more compounds

397 that are of higher molecular weight, more oxygenated, and of lower volatility (Figure 9b). The

398 SOA yields of many of these compounds are unknown, but the lower volatility and higher

399 oxygen content of the low-temperature profile suggests a potentially more efficient SOA

400 formation. We note that the compounds with $C_0 < 10^2$ µg m^{-3} shown in Figure 9b should be

401 primarily in the particle phase and not measureable by PTR-MS without long delay times

402 (Pagonis et al., 2017). However, the volatility of these compounds (calculated from the elemental

403 composition) has an uncertainty of several orders of magnitude. Also, the cyclic compounds that
404 are abundant in the low-temperature profile, such as aromatic oxygenates, produce
405 multifunctional ring-opening-products that are known to be efficient SOA precursors (Yee et al.,
406 2013). In a similar manner to the OH reactivity, the total volatility distribution can be estimated
407 from the relative importance of the high- and low-temperature pyrolysis in a given fire.

408

3.4 Relationship of fuel characteristics to relative importance of high- and low-temperature
pyrolysis factors

411 To use the PMF profiles (Figure 3) for estimates of VOC emissions from other fires, it is
412 necessary to know the relative fire-integrated contributions of high- and low-temperature
413 pyrolysis for those fires. As a step in this direction, in the present work, we found that fire-
414 integrated molar emission ratios of total VOCs from high-temperature pyrolysis to low-
415 temperature pyrolysis, $\sum VOC_{high-T}$ (in ppbv)/$\sum VOC_{low-T}$ (in ppbv), are related to which parts of
416 the plants are burned (blue bars in Figure 10). When leafy fuels (i.e., canopy, shrub, and
417 herbaceous fuels) are burned, the fraction of total VOC emissions originating from high-
418 temperature pyrolysis is higher than those from low-temperature pyrolysis. These results imply
419 that surface-to-volume ratios and the content of biopolymers in a given fuel can strongly affect
420 the relative importance of high- and low-temperature pyrolysis. Leaves have high surface-to-
421 volume ratios and despite higher fuel moisture, at least the surface may tend to heat up easily,
422 resulting in a higher contribution from the high-temperature factor. The higher monoterpene
423 content of foliage may explain why low-temperature distillation products like monoterpenes are
424 associated with the high-T pyrolysis factor.

425 In contrast, the burn of rotten wood was found to contain VOC emissions from low-
426 temperature pyrolysis only. Our brown rotten wood samples were enriched in lignin (Kirk and
427 Cowling, 1984). Lignin is relatively resistant to thermal decomposition compared to cellulose
428 and hemicellulose. The temperature range where pyrolytic decomposition occurs significantly is
429 280-500 °C for lignin, 240-350 °C for cellulose, and 200-260 °C for hemicellulose (Liu et al.,
430 2016; Babu, 2008), as shown in Figure 4b. In our laboratory fires, the rotten wood first
431 smoldered for an extended period, and then flames were observed. However, only the low-
432 temperature profile was observed. This suggests that it is more difficult for lignin-rich fuels to
433 reach high enough temperatures to emit the "high-temperature pyrolysis" VOCs. Therefore, we

434 do not see the same gradient in pyrolysis products that is observed for other fuel burns mainly

435 consisting of cellulose and hemicellulose. Nitrogen content and speciation also vary between

436 different biomass components, and temperature and differences in biopolymer content have been

437 shown to strongly affect the composition of nitrogen-containing emissions (Hansson et al., 2004;

438 Ren et al., 2011; Coggon et al. 2016). This is consistent with the observed differences in nitrogen

439 speciation between the two profiles.

440

441 **3.5 High- and low-temperature pyrolysis profiles describe total VOC emissions**

442   Previous studies have found a correlation between the emission factors of certain VOCs and

443 the fire-integrated modified combustion efficiency (MCE) (Yokelson et al., 1996: Yokelson et al.,

444 1997; Selimovic et al., 2017). Thus, one might expect that the high- and low-temperature

445 pyrolysis factors would also show a strong relationship to MCE. However, MCE does not

446 parameterize the relative amounts of high- and low-temperature pyrolysis products very well (red

447 bars in Figure 10).The basic reason is that the CO_2 emission is overwhelmingly from flaming

448 combustion, which is *not* the main source of most VOC emissions, and is not expected to

449 correlate with a linear combination of the high- and low-temperature pyrolysis processes, while

450 CO emissions are reasonably well correlated with an average of high- and low-temperature

451 emissions (Figure S6). CO_2 and the PMF profiles are not correlated in rotten wood burns. The

452 CO_2 emissions are enhanced by shifting from the smoldering to flaming combustion, but VOC

453 emission patterns are not changed from the low- to high-temperature pyrolysis (Figure S6).

454 Consequently, CO_2 and MCE, which indicate the separation between flaming and smoldering

455 combustions, are not appropriate to estimate the high-/low-temperature pyrolysis VOC

456 emissions .

457   Studies of laboratory burns and wildfires have reported variable emission ratios (or factors)

458 for various VOCs, even for similar fuel types. Here we investigate how well total VOC

459 emissions in biomass burning can be fit by the average VOC emission profiles (Figure 3) using

460 emission factors and ratios reported in the literature for laboratory and field burns (Gilman et al.,

461 2015; Stockwell et al., 2015; Akagi et al., 2011). When fitting the present high- and low-

462 temperature factors to the other biomass burning data, total VOC emissions can be described

463 with different relative fractions of the factors (Figure S7). For example, the best fit to a

464 laboratory study by Gilman et al. (2015), using fuels from southwestern, southeastern, and

465   northern U.S. (e.g., pine, spruce, fir, chaparral, mesquite, and oak), includes 32% high-
466   temperature and 68% low-temperature VOC emissions; for another laboratory study by
467   Stockwell et al. (2015) including several types of grass, spruce, and chaparral, 59% high
468   temperature and 41% low temperature; temperate forest fires reported by Akagi et al. (2011),
469   77% high temperature and 23% low temperature, while in the case of chaparral fires, 48% high
470   temperature and 52% low temperature. The fitting can be done with high correlation coefficient
471   ($r \geq 0.92$) for all the literature data (Figure S7). This is further evidence that at most two factors
472   can explain the majority of VOC variability.

473

474   **3.6 Emission of specific compounds**

475   **3.6.1 Distillation phase**

476   At the beginning of many burn experiments, a white smoke is visible immediately prior to
477   ignition. This "distillation phase" does not result from pyrolysis or combustion, but rather a
478   gradual heating and release of water and volatile compounds trapped within the biomass. This
479   phase of the fire was not distinguished by PMF. The distillation phase from coniferous fuels is
480   enriched in some compounds highly relevant to atmospheric chemistry, especially terpenes (Koss
481   et al., 2017). But this phase lasts only a short time (typically less than 10 seconds), in which only
482   a short spike in emissions is observed. Accordingly, PMF cannot capture this phase effectively
483   even if a large number of factors is chosen. As an exception, the distillation phase of Sage,
484   enriched in terpenes and a specific oxygenated monoterpene (camphor), can be distinguished as a
485   third PMF factor, because that phase lasted longer than 30 seconds in that fire. The reported
486   overall residual of 15% includes the poorly fitted distillation phase, and we stress that it typically
487   accounts for only a small portion of the overall emissions. Additionally, with the exception of
488   terpenes, the composition of the distillation profile is similar to that of the high-temperature
489   profile.

490   For some fuel burns other than coniferous fuels (e.g., Manzanita), VOC emissions during the
491   distillation phase are quite small, although distillation smoke is visible. In these cases, PMF
492   incorporates this phase into the low-temperature pyrolysis factor. There may be a relationship
493   between the VOC emission process coincident with distillation (low- or high-temperature) and
494   the presence of visible smoke. For instance, perhaps here the temperatures are low enough that
495   the compounds are able to re-condense into visible smoke.

496

3.6.2 Duff burn

497

A fourth factor can be resolved from the PMF analysis of duff burns. The distribution of

499 VOC structures and functionality in the duff emission profiles (Figure 11a) is similar to the low-

500 temperature pyrolysis profile (Figure 11b). The major difference is much higher emission of

501 aliphatic nitrogen-containing compounds: 56% more of these compounds are emitted per-ppbv

502 VOC in the duff profile than in the low-temperature profile. The additional emissions are mostly

503 nitriles and amides, especially hydrogen cyanide (HCN), acetonitrile, and acetamide. Pyrroles

504 and pyridines are also enhanced, but are much less abundant overall.

505 The organic portion of duff is enriched in nitrogen relative to other components of coniferous

506 fuels. The nitrogen to carbon ratio in the Subalpine fir duff (N:C ratio = 0.028 by weight) was a

507 factor of 2.1 higher than the average of other Subalpine fir components, and the Engelmann

508 spruce duff N:C ratio (0.022) was 1.3 times higher than other Engelmann spruce components.

509 Coggon et al. (2016), who investigated VOC emissions from the burning of herbaceous and

510 arboraceous fuels, also found that the nitrogen-containing fraction of VOCs emitted from

511 biomass burning increased with the nitrogen content of the fuel.

512 However, the nitrogen content cannot entirely explain why duff has a unique emission profile.

513 Other fuels, such as Ceanothus and Ponderosa pine litter, have similar N:C ratios (0.025, 0.024,

514 and 0.022, respectively) but are explained well by the 2-factor PMF solution consisting of high-

515 and low-temperature pyrolysis factors. The contradiction may be due to differences in the

516 speciation of nitrogen-containing organics. In woody and leafy fuels, proteins and amino acids

517 account for 80-85% of the organic nitrogen (Ren and Zhao, 2015). In soils, proteins account for

518 typically only 40% of organic nitrogen, and heterocyclic nitrogen compounds (pyrroles and

519 pyridines) account for 35% (Schulten and Schnitzer, 1997). Pyrolysis of nitrogen heterocycles

520 releases HCN, while proteins and amino acids may release more NH_3 (Leppälahti and Koljonen,

521 1995). This is consistent with the higher HCN and nitriles characteristic of the duff emission

522 profile.

523

3.6.3 Variation in specific VOCs between fuels

524

525   When comparing emission profiles of individual fuels to the average profiles shown in
526   Figure 3, there are some specific compounds whose emissions are notably higher ($> \times 5$) or lower
527   ($< \times 0.2$) than the average (Figure S4). Here we highlight several key features:

528   (i)   For Ponderosa/Lodgepole/Loblolly pines, Douglas/Subalpine firs, and Juniper, the
529   emission of benzoquinone ($C_6H_4O_2 \cdot H^+$, m/z 109.028) is quite low in the high-
530   temperature pyrolysis: 7-21% of the average emission for the pines and firs, and 2%
531   for Juniper (Figures S4a-1~4, 6, and 7).

532   (ii) For fuels other than coniferous fuels and Sage, i.e., Bear grass, Excelsior, Ceanothus,
533   Chamise, and Manzanita, emissions of monoterpenes ($C_{10}H_{16} \cdot H^+$, m/z 137.132) are
534   only 2-15% of the average (Figures S4a-8~14).

535   (iii) Excelsior emits especially low quantities of nitrogen-containing compounds,
536   especially nitriles (hydrogen cyanide, acetonitrile, acrylonitrile, and propane nitrile)
537   and pyridine, in the high-temperature pyrolysis (Figure S4a-9). This is because the
538   nitrogen content in Excelsior is significantly lower than other fuels. The Excelsior
539   N:C ratio (0.005 by weight) is 3.6 times lower than the average of other fuels (0.017
540          $\pm$ 0.006).

541   (iv) High-temperature pyrolysis of Ceanothus produces quite high emission of
542   benzofuran-type compounds (Figure S4a-10). Benzofuran ($C_8H_6O \cdot H^+$, m/z 119.049)
543   and methylbenzofuran and possibly its isomer such as cinnamaldehyde ($C_9H_8O \cdot H^+$,
544   m/z 133.065) are 5.5 and 10.1 times higher than the average, respectively.

545   (v)   Sage specifically emits camphor ($C_{10}H_{16}O \cdot H^+$, m/z 153.127) in high-temperature
546   pyrolysis (Figure S4a-15).

547   (vi) There are a limited number of exceptions in low-temperature profiles (Figure S4b).
548   This means that low-temperature pyrolysis gives almost identical VOC emissions,
549   independent of fuel types.

550

551   **4 Conclusions**

552   This work focused on interpretation of VOC emissions from biomass burning. We provided
553   an understanding of VOC variability based on known chemical and physical processes to release
554   VOCs from fires. We explained most of the observed variability between VOC emissions from
555   fuel types and over the course of a fire using just two emission profiles: (i) high-temperature

556 pyrolysis profile and (ii) low-temperature pyrolysis profile. The results are summarized as
557 follows:

1. The two profiles can explain the variability in VOC emissions composition between different fuel types and over the course of individual fires, with an average residual of < 15%.

2. The high-temperature profile is quantitatively similar between different fuel types ($r >$ 0.92), and likewise for the low-temperature profile.

3. The two profiles are significantly different in terms of VOC composition, volatility, and contributors to OH reactivity. The high-temperature pyrolysis profile is enriched in aliphatic unsaturated hydrocarbons, (polycyclic) aromatic hydrocarbons, terpenes (emitted from distillation), HCN, HNCO, and HONO. The resulting OH reactivity is primarily attributed to terpenes, aliphatic hydrocarbons, and non-aromatic oxygenates. The low-temperature pyrolysis profile is enriched in aromatic oxygenates, furans, and NH_3. The OH reactivity is contributed significantly by furans and aromatics.

4. The fire-integrated molar emission ratios of total VOCs from high-temperature pyrolysis to low-temperature pyrolysis are related to the biopolymer composition and surface-to-volume ratios of fuels. Higher surface-to-volume ratios lead to total VOC emissions enriched in products resulting from high-temperature pyrolysis than from those resulting from low-temperature pyrolysis.

5. The two VOC profiles can model previously reported VOC data for laboratory and field burns ($r \geq 0.92$).

6. MCE, which parameterizes flaming and smoldering combustion, is not appropriate to estimate the high-/low-temperature pyrolysis VOC emissions. This suggests that the high- and low-temperature pyrolysis profiles may provide information on emissions that is not accessible with a broader definition of smoldering combustion implicit in the use of MCE.

7. Duff burns emit a specific VOC profile which is similar to that of low-temperature pyrolysis, but additionally includes aliphatic nitrogen-containing compounds, especially HCN, acetonitrile, and acetamide.

585 Our framework provides a way to understand VOC emission variability in other laboratory and
586 field studies of biomass burning.

587   Future work should include a quantitative comparison of the VOC PMF results to
588 measurements of aerosol, inorganic gases, and organic species not measured by PTR-ToF-MS.
589 Such a comparison would help define the relationship between VOCs and characteristics of
590 primary organic aerosol (POA). We note that the primary aerosols have also been shown to have
591 distinct profiles that correlate with different pyrolysis and combustion processes in the fire
592 (Reece et al., 2017; Haslett et al., 2017).

593

594

595 **Acknowledgments**
596   K. Sekimoto acknowledges the Postdoctoral Fellowships for Research Abroad from Japan
597 Society for the Promotion of Science (JSPS) and a Grant-in-Aid for Young Scientists (B)
598 (15K16117) from the Ministry of Education, Culture, Sports, Science and Technology of Japan.
599 A. Koss acknowledges support from the NSF Graduate Fellowship Program. M. Coggon
600 acknowledges the Visiting Postdoctoral Fellowship from Cooperative Institute for Research in
601 Environmental Sciences (CIRES). V. Selimovic and R. J. Yokelson were supported by NOAA-
602 CPO grant NA16OAR4310100. J. de Gouw worked as a consultant for Aerodyne Research Inc.
603 during part of the preparation phase of this manuscript. We thank for support from NOAA AC4
604 external funding, and thank the USFS Missoula Fire Sciences Laboratory for their assistance and
605 cooperation. This work was also supported in part by NOAA's Climate Change and Health of the
606 Atmosphere initiatives.

607

608

609 **References**
610 Akagi, S. K., Yokelson, R. J., Wiedinmyer, C., Alvarado, M. J., Reid, J. S., Karl, T., Crounse, J.
611   D., and Wennberg, P. O.: Emission factors for open and domestic biomass burning for use in
612   atmospheric models, Atmos. Chem. Phys., 11, 4039-4072, https://doi.org/10.5194/acp-11-
613   4039-2011, 2011.
614 Alvarado, M. J., Wang, C, and Prinn, R. G.: Formation of ozone and growth of aerosols in young
615   smoke plumes from biomass burning: 2. Three-dimensional Eulerian studies, J. Geophys. Res.,
616   114 (D9), D09307, http://doi.org/10.1029/2008JD011186, 2009.

617 Alvarado, M. J., Lonsdale, C. R., Yokelson, R. J., Akagi, S. K., Coe, H., Craven, J. S., Fischer, E.
618   V., McMeeking, G. R., Seinfeld, J. H., Soni, T., Taylor, J. W., Weise, D. R., and Wold, C. E.:
619   Investigating the links between ozone and organic aerosol chemistry in a biomass burning
620   plume from a prescribed fire in California chaparral, Atmos. Chem. Phys., 15 (12), 6667-6688,
621   http://doi.org/10.5194/acp-15-6667-2015, 2015.

622 Atkinson, R. and Arey, J. Atmospheric degradation of volatile organic compounds, Chem. Rev.,
623   103 (12), 4605-4638, http://doi.org/10.1021/cr0206420, 2003.

624 Babu, B. V.: Biomass pyrolysis: a state-of-the-art review. Biofuels, Bioprod. Bioref., 2, 393-414,
625   http://dpo.org/10.1002/bbb.92, 2008.

626 Burling, I. R., Yokelson, R. J., Griffith, D. W. T., Johnson, T. J., Veres, P., Roberts, J. M.,
627   Warneke, C., Urbanski, S. P., Reardon, J., Weise, D. R., Hao, W. M., and de Gouw, J.:
628   Laboratory measurements of trace gas emissions from biomass burning of fuel types from the
629   southeastern and southwestern United States, Atmos. Chem. Phys., 10, 11115-11130,
630   https://doi.org/10.5194/acp-10-11115-2010, 2010.

631 Christian, T. J., Kleiss, B., Yokelson, R. J., Holzinger, R., Crutzen, P. J., Hao, W. M., Saharjo, B.
632   H., and Ward, D. E.: Comprehensive laboratory measurements of biomass-burning emissions:
633   1. Emissions from Indonesian, African and other fuels, J. Geophys. Res., 108 (D23), 4719,
634   http://doi.org/10.1029/2003JD003704, 2003.

635 Christian, T. J., Kleiss, B., Yokelson, R. J., Holzinger, R., Crutzen, P. J., Hao, W. M., Shirai, T.,
636   and Blake, D. R.: Comprehensive laboratory measurements of biomass-burning emissions: 2.
637   First intercomparison of open-path FTIR, and GC-MS/FID/ECD, J. Geophys. Res., 109 (D2),
638   D02311, http://doi.org/10.1029/2003JD003874, 2004.

639 Cicerone, R. J., and Zellner, R.: The atmospheric chemistry of hydrogen cyanide (HCN), J.
640   Geophys. Res., 88 (C15), 10689-10696, http://doi.org/10.1029/JC088iC15p10689, 1983.

641 Coggon, M. M., Veres, P. R., Yuan, B., Koss, A., Warneke, C., Gilman, J. B., Lerner, B. M.,
642   Peischl, J., Aikin, K. C., Stockwell, C. E., Hatch, L. E., Ryerson, T. B., Roberts, J. M.,
643   Yokelson, R. J., and de Gouw, J. A.: Emissions of nitrogen-containing organic compounds
644   from the burning of herbaceous and arboraceous biomass: Fuel composition dependence and
645   the variability of commonly used nitrile tracers, Geophys. Res. Lett., 43(18), 9903–9912,
646   doi:10.1002/2016GL070562, 2016.

647 Collard, F. X., and Blin, J.: A review on pyrolysis of biomass constituents: Mechanisms and
648   composition of the products obtained from the conversion of cellulose, hemicelluloses and
649   lignin, Renew. Sustainable Energy Rev., 38, 594-608,
650   http://doi.org/10.1016/j.rser.2014.06.013, 2014.

651 Donahue, N. M., Epstein, S. A., Pandis, S. N., and Robinson, A. L.: A two-dimensional volatility
652   basis set: 1. Organic-aerosol mixing thermodynamics, Atmos. Chem., Phys., 11, 3303-3318,
653   http://doi.org/10.5194/acp-11-3303-2011, 2011.

654 Gilman, J. B., Lerner, B. M., Kuster, W. C., Goldan, P. D., Warneke, C., Veres, P. R., Roberts, J.
655   M., de Gouw J. A., Burling, I. R., and Yokelson, R. J.: Biomass burning emissions and
656   potential air quality impacts of volatile organic compounds and other trace gases from fuels
657   common in the US, *Atmos. Chem. Phys.*, 15 (24), 13915-13938, http://doi.org/10.5194/acp-
658   15-13915-2015, 2015.

659 Haidar, N. F., Patterson, J. M., Moors, M., and Smith, W. T.: Effects of structure on pyrolysis
660   gases from amino acids, J. Agric. Food. Chem., 29 (1), 163-165,
661   http://doi.org/10.1021/jf00103a040, 1981.

662 Hansson, K.-M., Samuelsson, J., Tullin, C. and Åmand, L.-E.: Formation of HNCO, HCN, and
663   NH3 from the pyrolysis of bark and nitrogen-containing model compounds, Combust. Flame,
664   137 (3), 265–277, doi:10.1016/J.COMBUSTFLAME.2004.01.005, 2004.

665 Haslett, S. L., Thomas, J. C., Morgan, W. T., Hadden, R., Liu, D., Allan, J. D., Williams, P. I.,
666   Sekou, K., Liousse, C., and Coe, H.: Highly-controlled, reproducible measurements of aerosol
667   emissions from African biomass combustion, Atmos. Chem. Phys. Discuss.,
668   http://doi.org/10.5194/acp-2017-679, in review, 2017.

669 Hatch, L. E., Luo, W., Pankow, J. F., Yokelson, R. J., Stockwell, C. E., and Barsanti, K. C.:
670   Identification and quantification of gaseous organic compounds emitted from biomass
671   burning using two-dimensional gas chromatography–time-of-flight mass spectrometry, Atmos.
672   Chem. Phys., 15, 1865-1899, https://doi.org/10.5194/acp-15-1865-2015, 2015.

673 Houser, T. J., McCarville, and M. E., Biftu, T.: Kinetics of the thermal decomposition of
674   pyridine in a flow system, Int. J. Chem. Kinet., 12 (8), 555-568,
675   http://doi.org/10.1002/kin.550120806, 1980.

676 Jaffe, D. A., and Wigder, N. L.: Ozone production from wildfires: A critical review, Atmos.
677   Environ., 51, 1-10, http://doi.org/10.1016/j.atmosenv.2011.11.063, 2012.

678   Johnson, W. R., and Kan, J. C.: Mechanisms of hydrogen cyanide formation from the pyrolysis
679   of amino acids and related compounds, J. Org. Chem., 36 (1), 189-192,
680   http://doi.org/10.1021/jo00800a038, 1971.

681   Kirk, T. K., and Cowling, E. B.: Biological decomposition of solid wood, Adv. Chem., 207 (12),
682   455-487, http://doi.org/10.1021/ba-1984-0207.ch012, 1984.

683   Koss, A. R., Sekimoto, K., Gilman, J. B., Selimovic, V., Coggon, M. M., Zarzana, K. J., Yuan,
684   B., Lerner, B. M., Brown, S. S., Jimenez, J. L., Krechmer, J., Roberts, J. M., Warneke, C.,
685   Yokelson, R. J., and de Gouw, J.: Non-methane organic gas emissions from biomass burning:
686   identification, quantification, and emission factors from PTR-ToF during the FIREX 2016
687   laboratory experiment, Atmos. Chem. Phys. Discuss., https://doi.org/10.5194/acp-2017-924,
688   in review, 2017.

689   Leppälahti, J., and Koljonen, T.: Nitrogen evolution from coal, peat and wood during
690   gasification: Literature review, Fuel Process. Technol., 43, 1-45, http://doi.org/10.1016/0378-
691   3820(94)00123-B, 1995.

692   Li, Y., Pöschl, U., and Shiraiwa, M.: Molecular corridors and parameterizations of volatility in
693   the chemical evolution of organic aerosols, Atmos. Chem. Phys., 16 (5), 3327-3344,
694   http://doi.org/10.5194/acp-16-3327-2016, 2016.

695   Liu, W. -J., Li, W. -W., Jiang, H., and Yu, H. -Q.: Fates of chemical elements in biomass during
696   its pyrolysis, Chem. Rev., 117 (9), 6367-6398, http://doi.org/10.1021/acs.chemrev.6b00647,
697   2016.

698   Mackie, J. C., Colket, M. B., III, and Nelson, P. F.: Shock tube pyrolysis of pyridine, J. Phys.
699   Chem., 94 (10), 4099-4106, http://doi.org/10.1021/j100373a040, 1990.

700   Manion, J. A., Huie, R. E., Levin, R. D., Burgess D. R., Jr., Orkin, V. L., Tsang, W., McGivern,
701   W. S., Hudgens, J. W., Knyazev, V. D., Atkinson, D. B., Chai, E., Tereza, A. M., Lin, C. –Y.,
702   Allison, T. C., Mallard, W. G., Westley, F., Herron, J. T., Hampson, R. F., and Frizzell, D. H.:
703   NIST Chemical Kinetics Database, NIST Standard Reference Database 17, Version 7.0 (Web
704   Version), Release 1.6.8, Data version 2015.12, National Institute of Standards and
705   Technology, Gaithersburg, Maryland, 20899-8320. Web address: http://kinetics.nist.gov/,
706   last access: 28 November 2017, 2017.

707   Naeher, L. P., Brauer, M., Lipsett, M., Zelikoff, J. T., Simpson, C. D., Koenig, J. Q., and Smith,
708   K. R.: Woodsmoke health effects: A review, Inhal. Toxicol., 19 (1), 67-106,
709   https://doi.org/10.1080/08958370600985875, 2007.

710   NIST Chemistry WebBook, Web address: http://webbook.nist.gov/chemistry/, last access: 28
711   November 2017, 2017.

712   Paatero, P., and Tapper, U.: Positive matrix factorization: A non-negative factor model with
713   optimal utilization of error estimates of data values, *Environmetrics*, 5 (2), 111-126,
714   http://doi.org/10.1002/env.3170050203, 1994.

715   Paatero, P.: Least squares formulation of robust non-negative factor analysis, Chemometr. Intell.
716   Lab., 37 (1), 23-35, https://doi.org/10.1016/S0169-7439(96)00044-5, 1997.

717   Pagonis, D., Krechmer, J. E., de Gouw, J. A., Jimenez, J. L. and Ziemann, P. J.: Effects of gas-
718   wall partitioning in Teflon tubing and instrumentation on time-resolved measurements of gas-
719   phase organic compounds, Atmos. Meas. Tech., 10, 4687–4696, doi:10.5194/amt-2017-279,
720   2017.

721   Patterson, J. M., Tsamasfyros, A., and Smith, W. T.: Pyrolysis of pyrrole, J. Heterocycle Chem.,
722   5 (5), 727-729, http://doi.org/10.1002/jhet.5570050527, 1968.

723   Reardon, J.: Duff. *In:* FireWords: Fire Science Glossary [electronic]. U.S. Department of
724   Agriculture, Forest Service, Rocky Mountina Research Station, Fire Science Laboratory
725   (Producer). Available: http://www.firewords.net, last update 2007.

726   Reece, S. M., Sinha, A., and Grieshop, A. P.: Primary and photochemically aged aerosol
727   emissions from biomass cookstoves: Chemical and physical characterization, Environ. Sci.
728   Technol., 51 (16), 9379-9390, http://doi.org/10.1021/acs.est.7b01881, 2017.

729   Ren, Q., Zhao, C., Chen, X., Duan, L., Li, Y. and Ma, C.: NO_x and N_2O precursors (NH_3 and
730   HCN) from biomass pyrolysis: Co-pyrolysis of amino acids and cellulose, hemicellulose and
731   lignin, Proc. Combust. Inst., 33(2), 1715–1722, http://doi.org/10.1016/J.PROCI.2010.06.033,
732   2011.

733   Ren, Q., and Zhao, C.: Evolution of fuel-N in gas phase during biomass pyrolysis, Renew. Sust.
734   Energ. Rev., 50, 408-418, http://doi.org/10.1016/j.rser.2015.05.043, 2015.

735   Roberts, J. M, Veres, P. R., Cochran, A. K., Warneke, C., Burling, I. R., Yokelson, R. J., Lerner,
736   B., Gilman, J. B., Kuster, W. C., Fall, R., and de Gouw, J.: Isocyanic acid in the atmosphere

737 and its possible link to smoke-related health effects, Proc. Natl. Acad. Sci., 208 (22), 8966-
738 8971, http://doi.org/10.1073/pnas.1103352108, 2011.

739 Rumble, J. R. CRC Handbook of Chemistry and Physics, 98th Ed. (2017-2018).

740 Schulten, H. –R. and Schnitzer, M.: The chemistry of soil organic nitrogen: a review, Biol. Fert.
741 Soils., 26, 1-15, 1997.

742 Selimovic, V., Yokelson, R. J., Warneke, C., Roberts, J. M., de Gouw, J., Reardon, J., and
743 Griffith, D. W. T.: Aerosol optical properties and trace gas emissions by PAX and OP-FTIR
744 for laboratory-simulated western US wildfires during FIREX, *Atmos. Chem. Phys. Discuss.*,
745 http://doi.org/10.5194/acp-2017-859, in review, 2017.

746 Stockwell, C. E., Veres, P. R., Williams, J., and Yokelson, R. J.: Characterization of biomass
747 burning emissions from cooking fires, peat, crop residue, and other fuels with high-resolution
748 proton-transfer-reaction time-of-flight mass spectrometry, Atmos. Chem. Phys., 15 (15), 845-
749 865, http://doi.org/10.5194/acp-15-845-2015, 2015.

750 Ulbrich, I. M., Canagaratna, M. R., Zhang, Q., Worsnop, D. R., and Jimenez, J. L.: Interpretation
751 of organic components from Positive Matrix Factorization of aerosol mass spectrometric data,
752 Amos. Chem. Phys., 9 (9), 2891-2918, http://doi.org/10.5194/acp-9-2891-2009, 2009.

753 Yaws, C. L.: The Yaws Handbook of Vapor Pressure: Antoine Coefficients, Elsevier Science,
754 2015.

755 Yee, L. D., Kautzman, K. E., Loza, C. L., Schilling, K. A., Coggon, M. M., Chhabra, P. S., Chan,
756 M. N., Chan, A. W. H., Hersey, S. P., Crounse, J. D., Wennberg, P. O., Flagan, R. C., and
757 Seinfeld, J. H.: Secondary organic aerosol formation from biomass burning intermediates:
758 phenol and methoxyphenols, Atmos. Chem. Phys., 13 (16), 8019–8043,
759 http://doi.org/10.5194/acp-13-8019-2013, 2013.

760 Yokelson, R. J., Griffith, D. W. T., and Ward, D. E.: Open-path Fourier transform infrared
761 studies of large-scale laboratory biomass fires, J. Geophys. Res. Atmos., 101 (D15), 21067-
762 21080, http://doi.org/10.1029/96JD01800, 1996.

763 Yokelson, R. J., Susott, R., Ward, D. E., Reardon, J., and Griffith, D. W. T.: Emissions from
764 smoldering combustion of biomass measured by open-path Fourier transform infrared
765 spectroscopy, J. Geophys. Res. Atmos., 102 (D15), 18865-18877,
766 http://doi.org/10.1029/97JD00852, 1997.

767   Yokelson, R. J., Crounse, J. D., de Carlo, P. F., Karl, T., Urbanski, S., Atlas, E., Campos, T.,

768   Shinozuka, Y., Kapustin, V., Clarke, A. D., Weinheimer, A., Knapp, D. J., Montzka, D. D.,

769   Holloway, J., Weibring, P., Flocke, F., Zheng, W., Toohey, D., Wennberg, P. O., Wiedinmyer,

770   C., Mauldin, L., Fried, A., Richter, D., Walega, J., Jimenez, J. L., Adachi, K., Buseck, P. R.,

771   Hall, S. R., and Shetter, R.: Emissions from biomass burning in the Yucatan, Atmos. Chem.

772   Phys., 9 (15), 5785-5812, http://doi.org/10.5194/acp-9-5785-2009, 2009.

773   Yuan, B., Koss, A., Warneke, C., Gilman, J. B., Lerner, B. M., Stark, H., and de Gouw, J. A.: A

774   high resolution time-of-flight chemical ionization mass spectrometer utilizing hydronium ions

775   (H_3O^+ ToF-CIMS) for measurements of volatile organic compounds in the atmosphere,

776   Atmos. Meas. Tech., 9 (6), 2735-2752, http://doi.org/10.5194/amt-9-2735-2016, 2016.

777   Yuan, B., Koss, A., Warneke, C., Coggon, M., Sekimoto, K., and de Gouw, J. A.: Proton-

778   transfer-reaction mass spectrometry: Applications in atmospheric sciences, Chem. Rev., 117

779   (21), 13187-13229, http://doi.org/10.1021/acs.chemrev.7b00325, 2017.

780
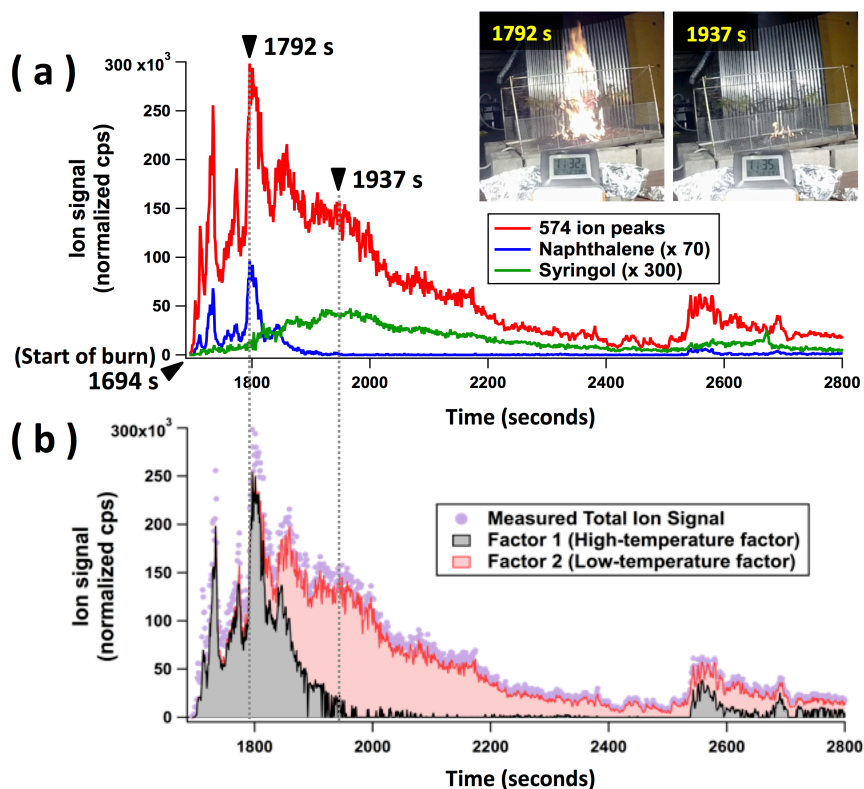
781

782

783 **Figure 1. Results for an example burn of Ponderosa pine realistic mixture (Fire #02). (a)**

784 **Time series of ion signals of 574 ion peaks, naphthalene ($C_{10}H_8 \cdot H^+$, *m/z* 129.070), and**

785 **syringol ($C_8H_{10}O_3 \cdot H^+$, *m/z* 155.070). (b) PMF results of 2-factor solution. The grey and pink**

786 **colors are stacked, not overlapped.**

787
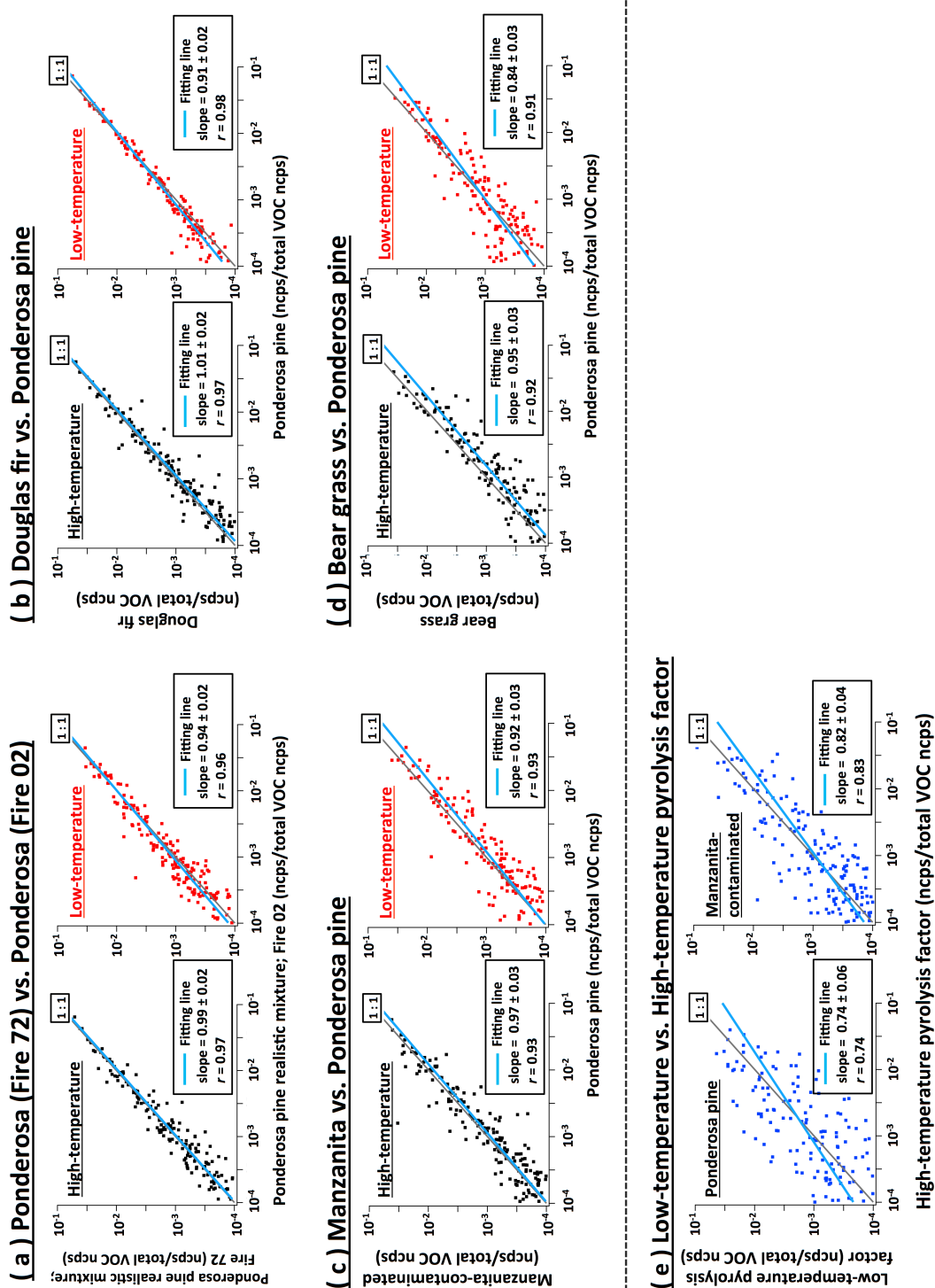
Figure 2. Comparison of mass spectral profiles: (a) Ponderosa pine realistic mixture (Fire #72) vs. Ponderosa pine realistic mixture (Fire #02) for high- and low-temperature pyrolysis factors. (In this case, PMF was separately performed for data of Fire #02 and #72.) (b) Douglas fir vs. Ponderosa pine for high- and low-temperature factors. (c) Manzanita (contaminated) vs. Ponderosa pine for both the factors. (d) Bear grass vs. Ponderosa pine for both the factors. (e) Low- vs. high-temperature pyrolysis factor for Ponderosa pine and Manzanita (contaminated). Data points in individual panels correspond to well-fitted 434 ion peaks. Correlation coefficient (r) is obtained using logarithmic fraction, i.e, log(ncps/total VOC ncps).
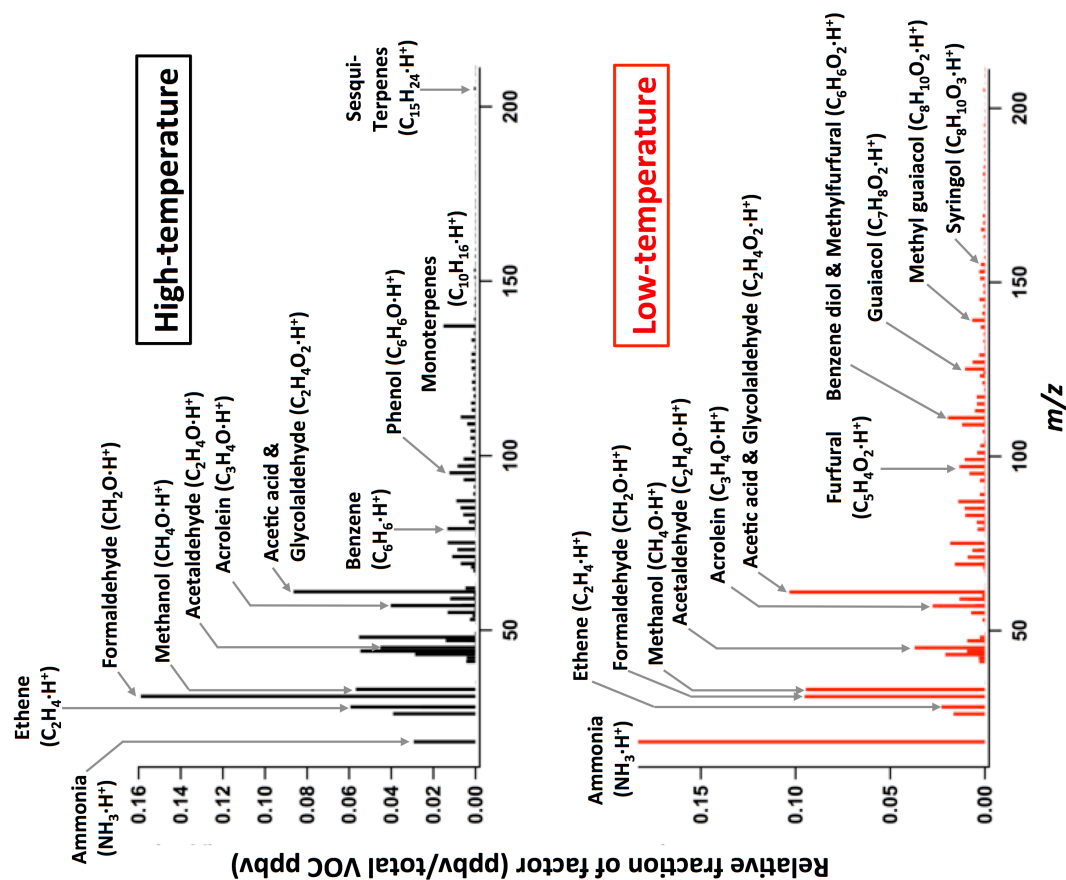
Figure 3. Average VOC emission profiles of high- and low-temperature pyrolysis factors, obtained using consolidated PMF results of 15 different fuels.
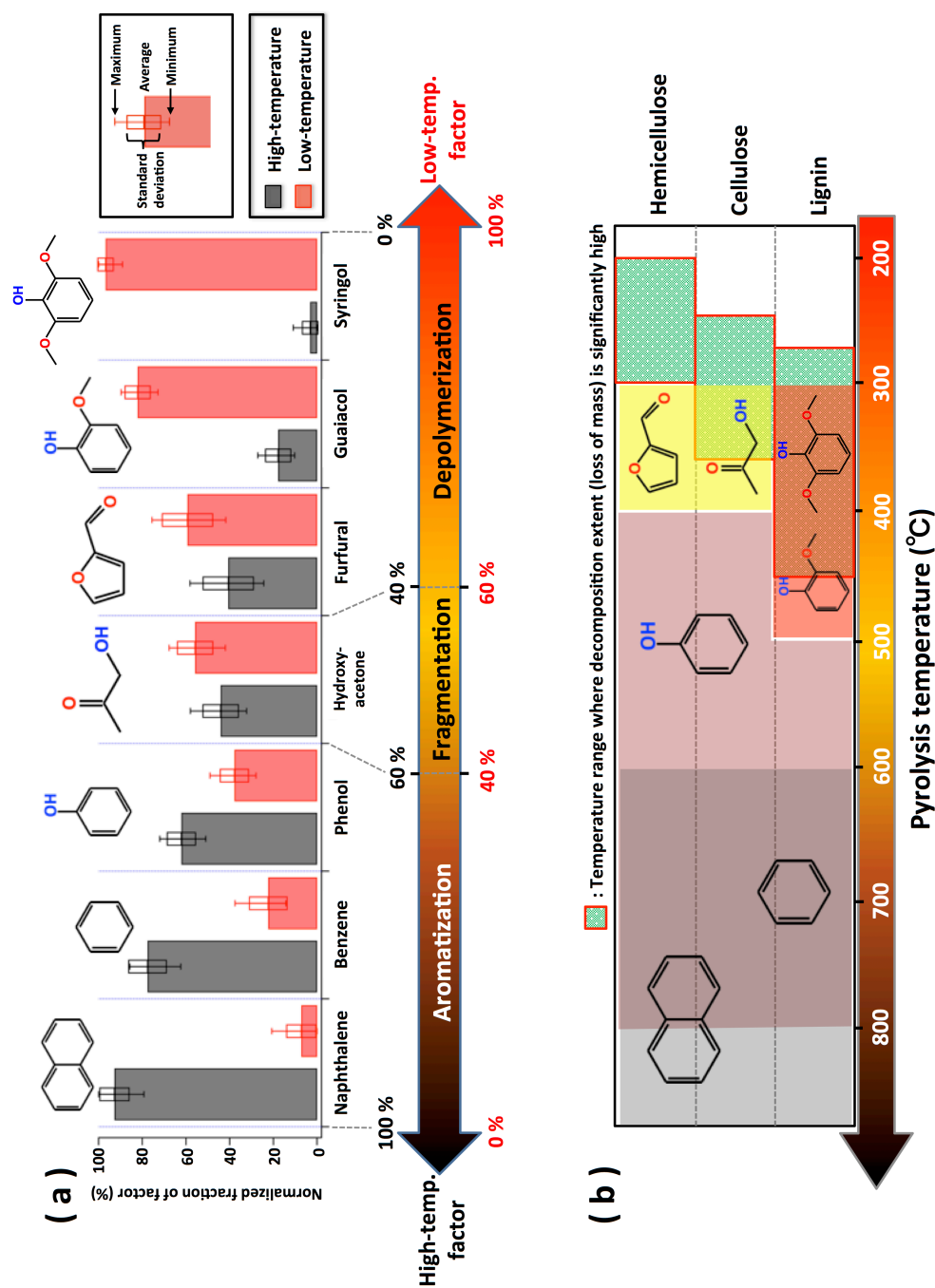
Figure 4. (a) Normalized fraction of factors for selected biomass pyrolysis products, obtained using PMF results of 15 different fuels. **(b)** Diagram of the relationship between pyrolysis temperature and products for hemicellulose, cellulose, and lignin.
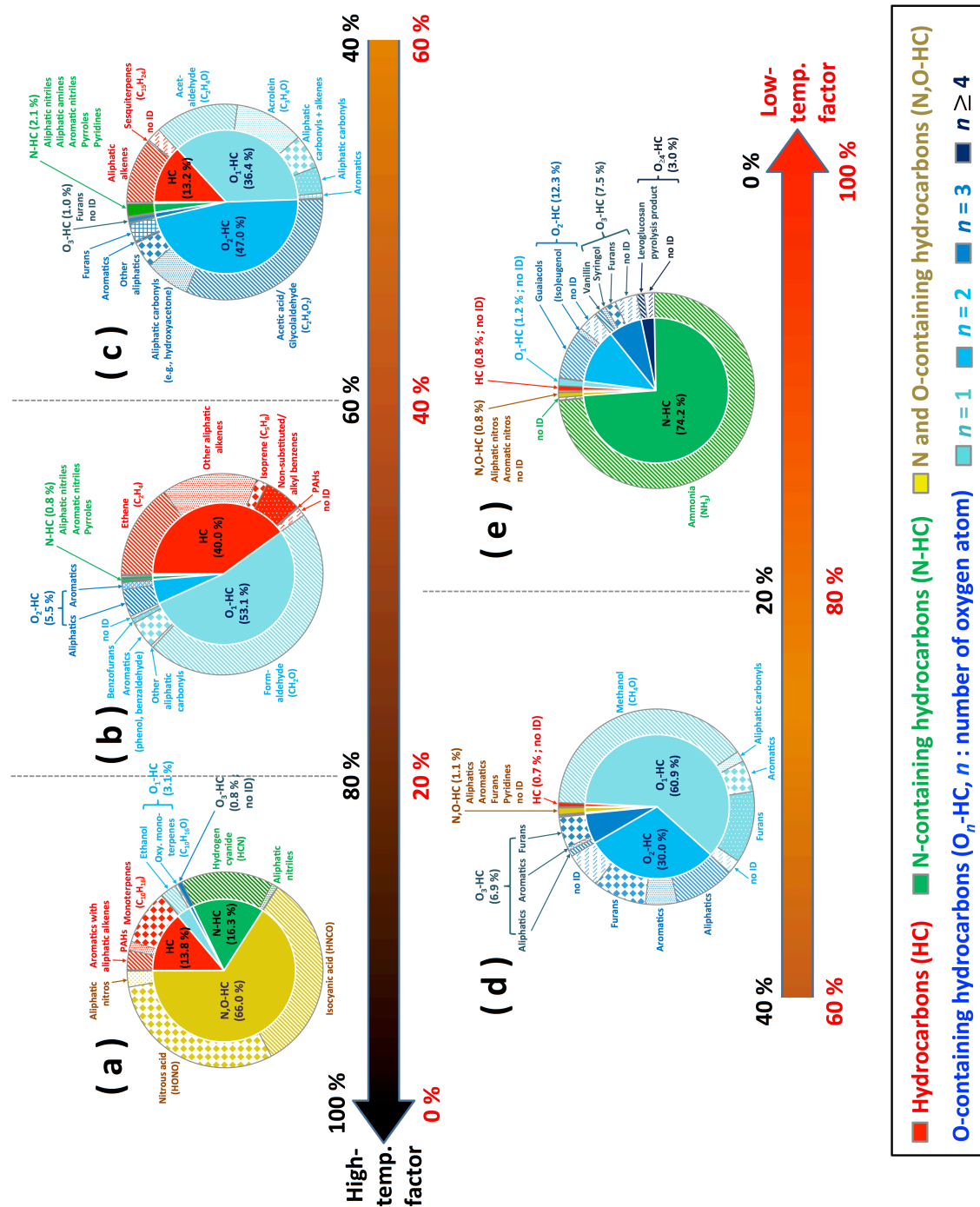
Figure 5. Contributions, shown as normalized fractions, of VOCs relative to the high- and low-temperature factors: (a) $F_{\text{High-T}}$ = 100-80% and $F_{\text{Low-T}}$ = 0-20%, (b) $F_{\text{High-T}}$ = 80-60% and $F_{\text{Low-T}}$ = 20-40%, (c) $F_{\text{High-T}}$ = 60-40% and $F_{\text{Low-T}}$ = 40-20% and (e) $F_{\text{High-T}}$ = 20-0% and $F_{\text{Low-T}}$ = 80-100%. In this figure, molar emissions (in units of ppbv) of all the ion peaks in VOC emission profiles (Figure 2b) are described. The inner circle in each pie chart shows the elemental composition of the emissions. The outer circle provides more detailed information on specific compounds, structures, and functionalities found in each group. Details of molar fractions in each category are summarized in Table S3.
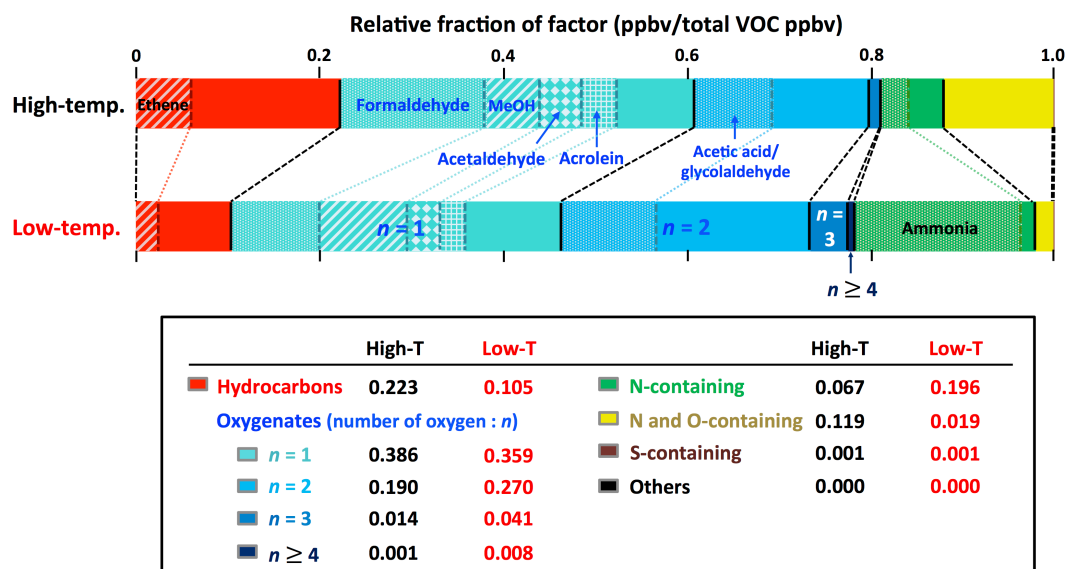
Figure 6. VOC composition in the high- and low-temperature emission profiles.
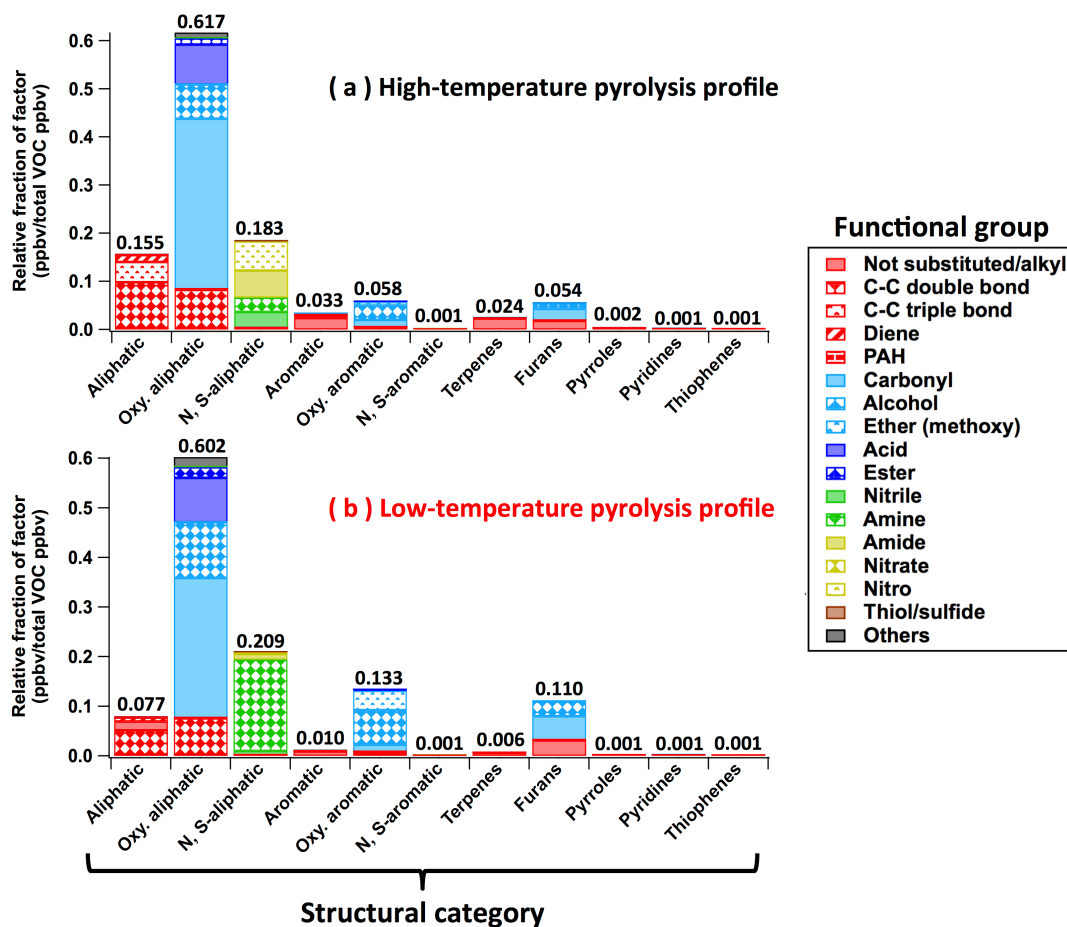
Figure 7. VOC composition in (a) high-temperature pyrolysis and (b) low-temperature pyrolysis emission profiles (Figure 3) sorted by 11 structural categories and 17 functional groups. Some VOCs have multiple structures. These are counted once in each relevant category. For example, benzofuran is counted in the structural categories of "Oxy. aromatic" and "Furans" as "Not substituted/alkyl" functional group. Structures detected with low abundance (<0.002 ppbv/total VOC ppbv) are mostly not-substituted or alkyl-substituted.
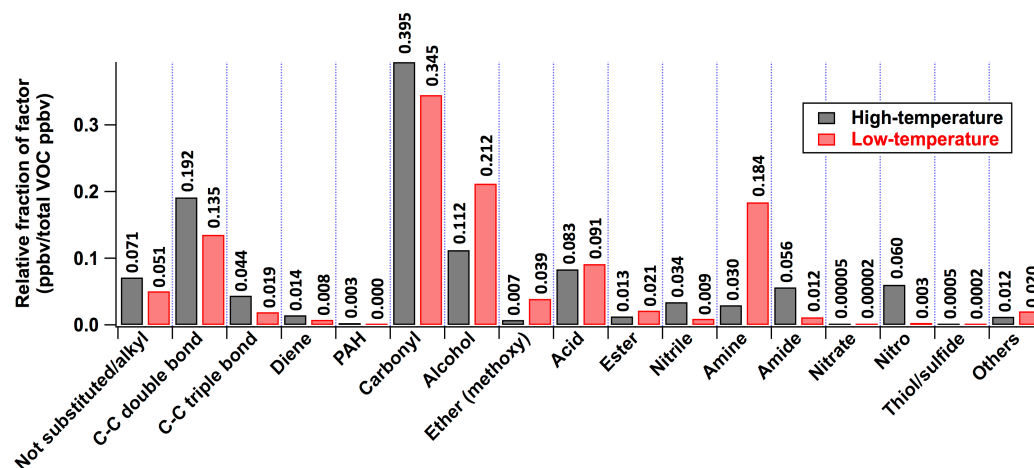
Figure 8. VOC composition in high- and low-temperature pyrolysis emission profiles (Figure 3) sorted by 17 functional groups. Each group includes various structures and elemental composition. Some VOCs have multiple functional groups. These are counted once in each relevant category. For example, guaiacol is counted in the categories of "Alcohol" and "Ether (methoxy)".
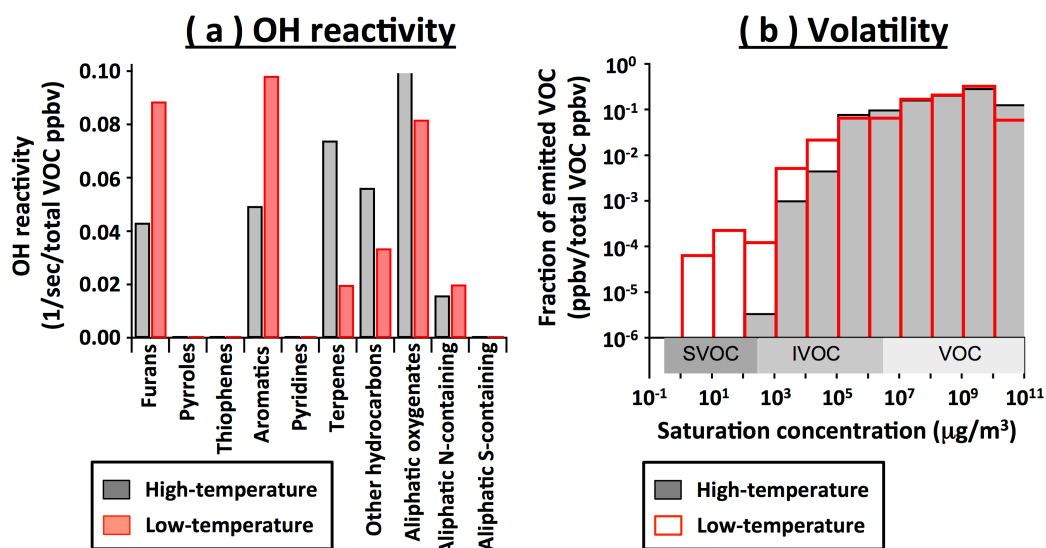
Figure 9. High- and low-temperature emission profiles compared by (a) OH reactivity and (b) volatility, described by saturation concentration (μg m^{-3}).
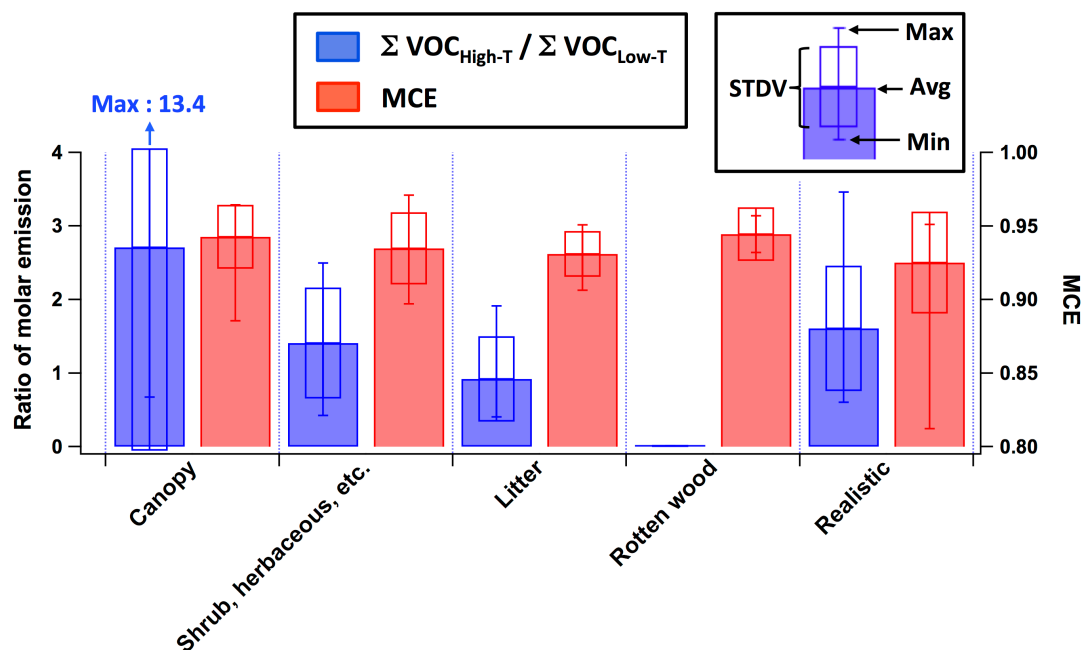
Figure 10. Ratios of fire-integrated molar emissions ("$\sum VOC_{High-T}/\sum VOC_{Low-T}$") or MCE for different type fuel parts, obtained using PMF results of 15 different fuels.

(a) VOC emission profile of duff burn
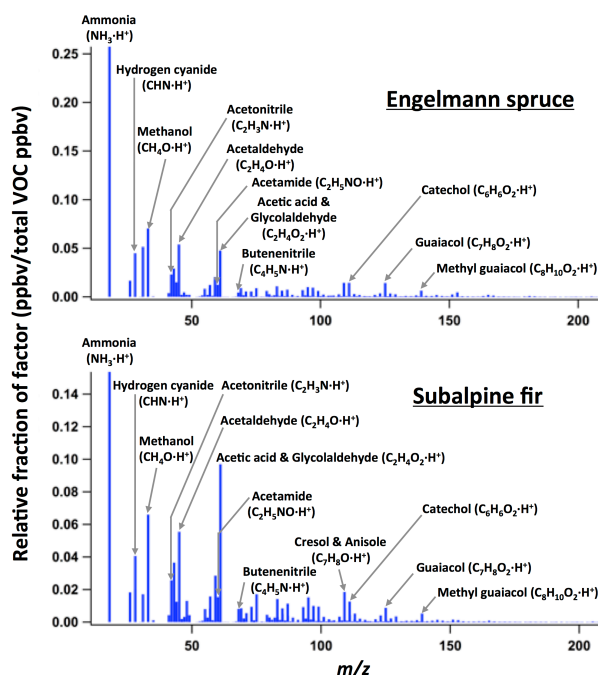
(b) Duff profile vs. Low-temp. profile
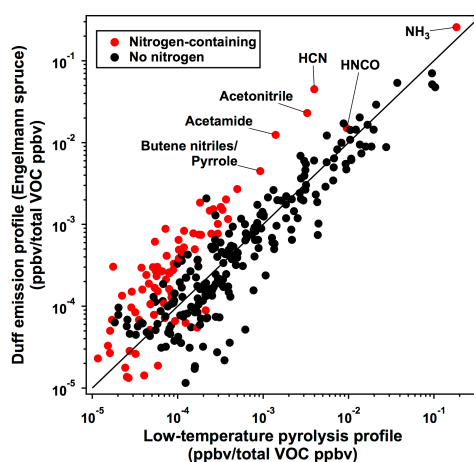
Figure 11. (a) VOC emission profile of duff burn of Engelmann spruce and Subalpine fir. (b) Scatter plot of duff emission profile (Engelmann spruce) versus average low-temperature pyrolysis profile.